HHS Public Access

Author manuscript

Brain Struct Funct. Author manuscript; available in PMC 2017 December 24.

Published in final edited form as:

Brain Struct Funct. 2017 December ; 222(9): 4051–4064. doi:10.1007/s00429-017-1451-x.

Co-altered Functional Networks and Brain Structure in Unmedicated Patients with Bipolar and Major Depressive Disorders

Hao He[1,2], **Jing Sui**[1,3,4,*], **Yuhui Du**[1], **Qingbao Yu**[1], **Dongdong Lin**[1], **Jian Yang**[5], **Wayne C. Drevets**[6], **Jonathan B. Savitz**[7], **Teresa A. Victor**[7], and **Vince D. Calhoun**[1,2,8,*]

[1]The Mind Research Network & Lovelace Biomedical and Environmental Research Institute, Albuquerque, NM, USA

[2]Electrical and Computer Engineering Department, University of New Mexico, Albuquerque, NM, USA

[3]Brainnetome Center and National Laboratory of Pattern Recognition, Institute of Automation, Chinese Academy of Sciences, Beijing, China

[4]CAS Center for Excellence in Brain Science and Intelligence Technology, Institute of Automation, Chinese Academy of Sciences, Beijing, China

[5]Beijing Engineering Research Center of Mixed Reality and Advanced Display, School of Optics and Electronics, Beijing Institute of Technology, 10081 Beijing, China

[6]Janssen Pharmaceuticals of Johnson & Johnson, Inc., Titusville, NJ, USA

[7]Laureate Institute for Brain Research, Tulsa, OK, USA

[8]Department of Psychiatry, Yale University, New Haven, CT, USA

Abstract

Bipolar disorder (BD) and major depressive disorder (MDD) share similar clinical characteristics that often obscure the diagnostic distinctions between these conditions. Both functional and structural brain abnormalities have been reported in these two disorders. However, the direct link between altered functioning and structure in these two diseases is unknown. To elucidate this relationship, we conducted a multimodal fusion analysis on the functional network connectivity (FNC) and gray matter density (GMD) from MRI data from 13 BD, 40 MDD, and 33 matched healthy controls (HC). A data-driven fusion method called mCCA+jICA was used to identify the co-altered FNC and GMD components. We found reduced GMD in the parietal and occipital cortices related to lower FNC in a sensory-motor network as well as stronger interconnection in frontal regions in BD compared to HC. Meanwhile, the MDD group exhibited GMD deficits in the amygdala and cerebellum. Among preliminary classifiers trained using features generated from these group discriminative components, the overall accuracy with resampling and cross-validation reached 91.3% for 3 groups and 99.5% for BD versus MDD. Our findings suggest that both

Address for Correspondence: Jing Sui, Vince D. Calhoun, The Mind Research Network, 1101 Yale Blvd, NE, Albuquerque, NM, 87106, jing.sui@nlpr.ia.ac.cn, vcalhoun@mrn.org.

overlapping and unique functional and structural deficits exist in BD and MDD, and the abnormalities may be utilized as potential diagnostic biomarkers.

Keywords

Bipolar disorders; Major depressive disorder; Functional network connectivity; Gray Matter density; Multimodal fusion; mCCA + jICA

Introduction

The major mood disorders, bipolar disorder (BD) and major depressive disorder (MDD, or unipolar depression), rank among the top illnesses worldwide causing disability and early death (Lancet 2015; Salomon et al. 2012). However, differentiating BD and MDD poses a major clinical challenge due to the high prevalence of similar symptoms (Angst et al. 2010; Judd et al. 2012). Objective markers derived from neuroimaging hold the potential to increase the accuracy of differentiating between BD and MDD patients to an extent that may improve the clinical and functional outcomes for individuals suffering from these disorders (de Almeida and Phillips 2013). In the decade both functional (Cerullo et al. 2014; Delvecchio et al. 2012) and structural (Kempton et al. 2011; Konarski et al. 2008) brain abnormalities in BD and MDD have been extensively studied in the magnetic resonance imaging (MRI) literature, however, few studies focused on data-driven, multimodal fusion techniques that exploit the complementary information between fMRI and sMRI in order to differentiate the two mood disorders.

Functional connectivity (FC) assessed from functional MRI (fMRI) captures the temporal coherence of blood oxygenation level dependent (BOLD) signal fluctuations in functionally-related gray matter regions that putatively reflect spontaneous neural activity (Biswal et al. 1995; Friston 2002). Recently, several studies have explored the differences in FC between BD and MDD using resting-state (Ellard et al. 2015; Goya-Maldonado et al. 2016; Marchand et al. 2013; Wang et al. 2015) or task-related fMRI (Anand et al. 2009; Redlich et al. 2015; Satterthwaite et al. 2015). We previously studies compared neuroimaging data between BD and MDD by constructing the functional network connectivity (FNC), composed of a whole brain graph with nodes defined by independent components analysis (ICA) (Jafri et al. 2008). We found that the FNC in BD was characterized by more closely connected and more efficient topological structures compared to MDD (He et al. 2016).

During neurodevelopment the formation of gyral folding patterns within the cerebral cortex is thought to reflect the anatomical connections between distinct cortical areas, which in turn relate to cerebral function (Poldrack 2010; Van Essen and Dierker 2007). This relationship between brain structure and function has been supported by previous neuroimaging studies (Greicius et al. 2009; Mars et al. 2011; van den Heuvel et al. 2009). However, the relationship between altered brain function and structure in mood disorders remains unclear. Generally, each neuroimaging modality provides a certain perspective on brain function or structure. However, data fusion through a joint analysis not only capitalizes on the strengths of each imaging modality, but also reveals underlying inter-relationships, potentially providing a more comprehensive understanding of brain deficits in psychiatric disorders

(Calhoun et al. 2006; Calhoun and Sui 2016; Sui et al. 2012a). To date, few studies of BD and MDD have assessed multimodal brain imaging data collected from the same subject sample. A conventional multimodal practice is firstly to analyze each modality separately, and then to compare at the results level (Rigucci et al. 2010). However, such an approach cannot capture directly the joint information available in multimodal imaging data (Calhoun and Sui 2016; Sui et al. 2012a). In a classification analysis on BD and MDD, Jie et al (Jie et al. 2015) utilized a machine learning model to select multimodal diagnostic discriminating features from combined fMRI and structural MRI (sMRI) data. Nevertheless, the joint function-structure changes that span across fMRI and sMRI in BD and MDD have not been characterized previously.

In this study, we utilized the resting-state FNC generated from our prior study as characteristics of fMRI. At the same time, gray matter densities (GMD) from the same subject samples were acquired using sMRI. In order to identify the co-altered networks across modalities, we assume that 1) whole brain FNC is a linear mixture of sources in the form of multiple sub-networks (Park et al. 2014), 2) whole brain GMD can also be linearly separated into a number of sources as spatial independent components (Xu et al. 2009), and 3) disorder incurred functional and structural brain changes are correlated across the source factors of modalities. A joint analysis was applied to FNC and GMD using a data fusion approach called multi-set canonical correlation analysis + joint independent component analysis (mCCA+jICA) (Sui et al. 2010; Sui et al. 2012b). We expected that the analysis which incorporates FNC and brain structure would reveal changes specific to BD or MDD, and that the abnormalities defined using this approach ultimately may served as potential diagnostic biomarkers with the potential to discriminate these two mood disorders.

Materials and Methods

Subjects

Resting-state fMRI and sMRI data were collected from 13 BD, 40 MDD, and 33 HCs at the Laureate Institute for Brain Research, Tulsa, OK, USA. The subjects in the three groups were comparable in age and gender (Table 1). The study received institutional ethical review board approval, and all subjects provided written informed consent to participate. The diagnoses of BD and MDD were established using the Structured Clinical Interview for the DSM by trained raters and confirmed by an unstructured interview with a psychiatrist. All patients included were either treatment naive or had discontinued prescribed medications on their own during at least the 3 weeks (8 weeks for fluoxetine) prior to scanning.

Data Acquisition

All images were collected on a GE Discover MR750 3-Tesla scanner with a 32-channel radio frequency coil. During the fMRI scan, participants were instructed to keep their eyes open and to not fall asleep. The resting-state scan lasted 6.4 min (191 volumes). T2*-weighted functional images were acquired using a gradient-echo EPI sequence with TE = 27 ms, TR = 2 s, flip angle = 78°, slice thickness = 2.9 mm, field of view = 240 mm, matrix size = 96×96. For structural scans, T1 images were acquired using a gradient-echo MP-RAGE

sequence with TE = 2.008 ms, TR = 5 s, flip angle = 8°, slice thickness = 0.9 mm, field of view 240 mm, matrix size = 256×256.

Preprocessing

For the fMRI data, the first seven volumes were excluded from analysis to allow for T1 equilibration. The SPM8 software package (http://www.fil.ion.ucl.ac.uk/spm/software/spm8) was employed to perform fMRI preprocessing on the remaining volumes. The images were first realigned using INRIalign (Freire et al. 2002), and were then spatially normalized to the standard Montreal Neurological Institute (MNI) space, resampled to 3 × 3× 3 mm^3 voxels using the nonlinear (affine + low frequency direct cosine transform basis functions) registration implemented in SPM8 toolbox. The imaging data were smoothed using a Gaussian kernel with a full-width at half-maximum of 8 mm.

Gray Matter Segmentation—Structural data were preprocessed using the SPM8 software package, such that each subject's brain image was segmented into white matter, gray matter, and cerebral spinal fluid with unmodulated normalized parameters via the unified segmentation method (Ashburner and Friston 2005). After segmentation, the images of GMD were smoothed to a full-width half maximum (FWHM) Gaussian kernel of 8 mm (White et al. 2001) and resliced to a matrix of 53 × 63 × 46 voxels. The preprocessed GMD served as the feature of sMRI for the following multimodal fusion analysis.

Functional Network Connectivity—Group ICA was performed on the preprocessed fMRI data using GIFT software (http://mialab.mrn.org/software/gift) (Calhoun and Adali 2012), resulting in 75 group independent components (ICs). Forty-eight ICs were characterized as intrinsic connectivity networks (ICNs) after removing ICs with artifacts following (Allen et al. 2011). The time courses (TCs) of 48 ICNs across whole brain were post-processed by detrending, regressing out head motion, despiking and low-pass filtering (<0.15 Hz). Then, the FNC for each subject was calculated as the absolute Pearson's correlation between TCs of each pair of ICs. The magnitude (absolute value) of functional network connectivity strength was used as the fMRI data feature to input into the multimodal fusion analysis. For more details of FNC feature generation, please refer to our previous publication (He et al. 2016).

mCCA+jICA Fusion Framework

The overall procedure of multimodal fusion on functional and structural imaging modalities is illustrated in Figure 1. In mCCA+jICA framework, we assume an n-modal ($n = 2$ in our case) set X_k as a linear mixture of M sources given by S_k, with a non-singular mixing matrix A_k for each modality k, that is:

$$\boldsymbol{X_k}=\boldsymbol{A_k}\boldsymbol{S_k}, k=1, 2, \ldots, n \quad (1)$$

In this study, the component number M was set to be 8 estimated using a modified MDL method (Li et al. 2007).

Typically, the number of data points per subject L_k in X_k is much larger than subject number N. For each modality k, X_k is a $N \times L_k$ feature matrix, and S_k is a $M \times L_k$ matrix. The underlying sources S_k are distinct within each dataset. The columns of A_i and A_j have higher correlation only on their corresponding indices, with modality $i,j \in \{1,2, \ldots, n\}$, $i \neq j$.

In this study, we utilized the FNC map as feature X_1 for functional MRI, and non-zero values in GMD as feature X_2 for structural MRI. The multi-set Canonical Correlation Analysis (mCCA)(Li et al. 2009) was first applied to the input dataset, generating two linked canonical variates (CVs) D_k by maximizing the inter-subject covariation across two sets of features. The resulting CVs D_k were sorted by correlation to match to the potential correlated mixing profiles between components of each modality, as shown in Figure 1. However, the sources of associated maps C_k (in $M \times L_k$) may not be completely separated and reconstructed. Joint ICA (jICA) were then adopted on the concatenated maps $[C_1, C_2]$ to obtain the final maximally independent source S_k and corresponding whitening matrix W. The final mixing profiles A_k can be achieved by multiplying the mixing matrices of each step, $A_k = D_k W^{-1}$.

Statistical testing on group abnormalities

To reduce the age and gender effects, we regressed out the subjects' age and gender as covariates from mixing profiles A_k, and performed statistical tests on residuals $\boldsymbol{A_k}'$. Analysis of variance (ANOVA) and two-sample t–tests were performed on mixing coefficients $\boldsymbol{A_k}'$ of each IC for each modality k, to reveal the components that have significant group difference among subjects. Any component of the same index that showed significant group difference in both modalities was considered a modality-common (or joint) group-discriminative IC. In contrast, any group difference of one component that occurred in a single modality was considered a modality-specific group-discriminative IC. These ICs were termed joint or distinct abnormalities respectively. The false discovery rate (FDR) correction (Benjamini and Hochberg 1995) for multiple testing was applied to the p-values obtained from the statistical tests.

Identifying Community Structures and Hubs

ICs of FNC correspond to the connectivity weights of multiple edge-sharing sub-networks within the brain (Park et al. 2014). To better capture the characteristics of the sub-networks that showed a group difference, those FNC components were further analyzed using graph theory. Modular community structure has been repeatedly demonstrated in resting state functional brain connectivity networks. The brain regions that are functionally associated and subserve similar roles may be divided into a same module during the modular analysis. In particular, the brain nodes that are highly connected with other regions in the same module are called hubs (Rubinov and Sporns 2010).

To assess the modular community structures and hubs, the connectivity weights of FNC subnetworks were first rescaled into [−1, 1]. A fine-tuned Louvain algorithm (Reichardt and Bornholdt 2006; Ronhovde and Nussinov 2009) from the brain connectivity toolbox was adopted to discover the optimal community structure of the FNC subnetworks, which divide

the graph into non-overlapping groups of nodes (modules) in a way that maximizes the number of within-group edges, and minimizes the number of between-group edges.

Highly connected node within a module q could be identified by measuring of intra-module connectivity. Intra-module connectivity of node i, k_i^q is given by the sum of connectivity strengths S_{ik} with all other nodes in module q:

$$k_i^q = \sum_{k \in q} S_{\mathrm{ik}} \quad (2)$$

The z-score (Guimera and Amaral 2005)of node i is defined as

$$z_i = \frac{k_i^q - \overline{k}_q}{\sigma_q} \quad (3)$$

where $\bar{k}_q$ and σ_q are the mean and standard deviation of k_k^q for all nodes in module q. Nodes with higher z-scores are more strongly connected to the other nodes in the same module. In this study, we define a node with $z_i > 1.0$ as a hub (Yu et al. 2011). The BrainNet Viewer toolbox (http://www.nitrc.org/projects/bnv/) was used for visualizing FNC subnetworks (Xia et al. 2013).

Classifications Based on the Features Selected

For the identified group-discriminative components, we further tested their potential use for disease classification (Figure 2). For each modality, we normalized (subtracted by mean then divided by standard deviation) each IC with significant group difference into z-values, which then were thresholded (FNC at $|z| > 2.0$, and GMD at $|z| > 3.0$) to generate a mask from each modality. The masks of the same modality then were combined and applied to the raw input data of each modality, which served as the input used to further classify 3 BD, MDD, and HC based on uni-modal and multi-modal features.

For comparison, we evaluated classifiers based on the features from the individual modality (FNC or GMD only), as well as combined features from both modalities (FNC+GMD). Classifiers were built and tested on the Weka 3.6 platform (http://www.cs.waikato.ac.nz/ml/weka/)(Witten et al. 2011). In order to balance the sample numbers in each group, the instances of BD group were resampled using a Synthetic Minority Oversampling TEchnique (SMOTE) (Chawla et al. 2002) to generate 39 BD samples. Each sample was assigned a class label based on its corresponding diagnostic group (BD, MDD or HC). We then trained four different classifiers: 1) Sequential Minimal Optimization for Support Vector Machine (SMO) (Keerthi et al. 2001), 2) Naïve Bayes (John 1995), 3) Random Forest (Breiman 2001), and 4) K-nearest neighbors (kNN) (Aha et al. 1991) where $k = 5$. To ensure stable performance of each classifier, stratified ten-fold cross validation was repeated 1000 times, yielding 10000 testing accuracy rates. For every ten-fold cross validation run, the samples were assigned into 10 groups randomly. In Iteration (Fold) (k =1,2, …, 10), group k was left out as testing cases towards the classifier model that was trained on other nine groups. Since

distinguishing BD and MDD is a major clinical challenge, the classification process was applied to distinguish all 3 groups as well as the BD and MDD groups only.

Results

Group Difference on Mixing Profiles

One joint group-discriminative IC (IC5) and one modality-specific group-discriminative IC (GMD-IC2) were detected, as shown in Figure 3, based on the statistical tests of the mixing coefficients derived from mCCA+jICA.

ANOVA on IC5 revealed significant group difference in both FNC ($p = 0.011$, FDR corrected) and GMD ($p = 0.006$, FDR corrected). In FNC-IC5, the subnetwork comprised of reduced functional connectivity magnitude (less correlated BOLD activity) in the superior parietal lobe (SPL), precentral gyrus (PreCG), postcentral gyrus(PoCG), middle temporal gyrus(MTG) and middle occipital gyrus(MOG) and cerebellum, but increased connectivity magnitude within regions associated with the superior frontal gyrus (SFG), precuneus, middle frontal gyrus (MFG), inferior parietal lobe (IPL), and limbic subcortical networks. GMD-IC5 corresponds to gray matter density in the SPL and MOG. A significant group difference was also found in GMD-IC5 between BD and HC in t-test ($p < 0.001$, FDR corrected, BD < HC). At the same time, pair-wise t-test indicated difference in FNC-IC5 between BD and HC ($p = 0.027$, uncorrected, BD < HC) and in GMD-IC5 between BD and MDD ($p = 0.014$, uncorrected, BD < MDD). However, these two p-values did not remain significant after correction for multiple testing (FDR). The correlation of mixing profiles between FNC and GMD was $r = 0.23$ ($p = 0.032$, uncorrected), indicating the changes within this component found in FNC and GMD are related across patients with BD.

IC2 showed a significant group difference in GMD only ($p = 0.004$, FDR corrected), which included cerebellum, amygdala and hippocampus. Both MDD and BD showed lower GMD than HC in this component, as shown in Figure 3 (MDD-HC: $p = 0.023$, FDR corrected; BD-HC: $p = 0.037$, uncorrected).

Community Structures and Hubs of FNC Component

In the FNC component that showed significant group difference (IC5), three non-overlapping modules were identified by fine-tuned Louvain algorithm, including two major community modules with nodes that are strongly interconnected together and a module that include nodes relatively isolated to others, as shown in Figure 4. Specifically, Module 1 contains 20 nodes intensively connected within default-mode (SFG and precuneus), cognitive control (MFG and IPL), and limbic subcortical networks. Module 2 comprised of 18 nodes, mostly in somatomotor networks (SPL, PreCG and PoCG), cerebellum, and visual networks (MTG and MOG). The remaining 10 nodes that are less closely connected were separated into Module 3.

It noteworthy that the connectivity weight of the subnetwork in Modules 1 and 2 were opposite in valence (orange for positive and cyan for negative weights in Figure 4), indicating subjects with higher connectivity strength magnitudes in one module have lower FC magnitudes in the other. Moreover, the mixing profile of FNC-IC5 in the BD group was

lower than in the HC group, which suggested that the BD group manifest a more densely interconnected Module 1 but less interconnected Module 2 comparing to HC in this subnetwork. Interestingly, this dual modular parcellation corresponded to two major areas organized from a recent resting-state FC study (Stoddard et al. 2016), which was based on a different approach of clustering voxel-wise connectivity.

Seven hubs were identified in the modular structure of FNC-IC5, including two hubs (MFG and SFG) in Module 1, four hubs (MTG, SPL, right PoCG, and left MOG) in Module 2, and one hub (SFG) in Module 3. These seven hubs are highlighted as larger nodes in Figure 4, indicating these brain regions play important roles in the altered FNC structure, and link to the abnormal GMD in BD.

Classifications

The average and standard deviation of 1000 accuracy rates of both 3-group and BD-MDD classification are shown in Figure 5. SMO performed best among 4 algorithms tested: averaged accuracy reached 91.3±8.1% for 3-group classification and 99.5±2.9% for distinguishing between BD and MDD using features from both modalities. For each of 4 algorithms, we also compared results of classifier trained using either unimodal or multimodal features. Overall, training with multimodal features achieved best or close to best accuracy with all algorithms.

Discussion

In this study, we conducted fusion analysis on functional and structural MRI data by applying mCCA+jICA framework to whole brain FNC and GMD. We aimed to identify abnormalities spanning across multiple imaging modalities and to evaluate the feasibility accuracy of these biomarkers to distinguish BD and MDD. Both modal-specific and modal-common components were identified. Further analysis on the group-discriminating FNC component revealed community structure and hubs, which conceivably may be associated with the mechanisms that are distinct to each disorder.

Functional and Structural Co-alterations in BD

IC5 showed significant group differences in both FNC and GMD, and t-tests found abnormalities are mostly in BD. From the spatial maps, IC5 in both modalities highlighted parietal and occipital lobes. Generally, the parietal lobe is commonly considered to be involved in processing tactile and proprioceptive information, language comprehension, speech, writing, and aspects of spatial orientation and perception. At the same time, the occipital lobe includes regions that are involved in visual perception and processing (Nolte 2009). Several sMRI studies showed significant reductions gray matter density and volume in BD subjects versus controls in the parietal lobe (Doris et al. 2004; Frazier et al. 2005; Lyoo et al. 2004; Lyoo et al. 2006) and the occipital lobe (Doris et al. 2004; Lochhead et al. 2004; Lyoo et al. 2006). Our results of GMD-IC5 thus appear consistent with these findings.

Earlier studies proposed the cortical thinning in sensory association cortices may be related to impairments in visual spatial neuropsychological function within BD subjects (Ferrier et al. 2004; Sweeney et al. 2000). As a joint-discriminative IC in our study, IC5 confirmed that

the reduced GMD in the parietal and occipital cortices were related with the alterations in cerebral function in the BD group. According to graph theory, the hub nodes of a module interact actively with other brain components, facilitate functional integration, and participate in module organization (Rubinov and Sporns 2010). The four hubs of Module 2, including two hubs in the parietal lobe, one in the temporal lobe, and one in the occipital lobe, were spatially distribute across different somatomotor and visual areas, indicating the abnormalities may have widespread effects in the function of sensory association cortices. Based on analysis of FNC-IC5, the parietal, occipital, temporal, and cerebellar fusiform areas were categorized into Module 2 with reduced connectivity in BD, demonstrating the direct correspondence of structural and functional deficits in this disorder.

In Module 1, the two hubs along with majority of implicated nodes were located within the prefrontal cortex. The prefrontal regions, including the orbitofrontal cortex (OFC), the anterior cingulate cortex (ACC), and the dorsomedial (DMPFC), dorsolateral (DLPFC) and ventrolateral (VLPFC) areas of the prefrontal cortex have been consistently implicated in cognitive control processes (Sui et al. 2015), including decision-making and emotion regulation (Kupfer et al. 2012; Phillips et al. 2008). In mood disorders, these prefrontal cortical areas form part of the limbic–cortical–striatal–pallidal–thalamic circuits that are hypothesized to be dysfunctional in MDD and BD based on neuroimaging studies (Drevets 2000; Price and Drevets 2012). A number of previous studies of resting-state FC in BD samples found increased resting-state FC in the prefrontal cortices, particularly within ventral prefrontal cortex in BD (Chepenik et al. 2010). Another ICA-defined FNC analysis reported that BD subjects showed increased FC in emotion evaluation regions such as the bilateral medial prefrontal cortex, and in “affective working memory network” including the DLPFC and VLPFC, during an affective working memory task (Passarotti et al. 2012). Abnormal medial prefrontal cortex connectivity between ICA components were also found during the resting-state in the BD group in multiple previous studies (Calhoun et al. 2011; Ongur et al. 2010). Our findings with stronger FC in BD subjects within the prefrontal cortical areas highlighted in Module 1 not only replicated our recent results on the same dataset with different analysis approaches (He et al. 2016), but also are in line with prior resting-state FC studies.

Another interesting finding was that two subcortical regions (Figure 4), the putamen and thalamus, were grouped together into Module 1, potentially consistent with the anatomical circuits formed between the prefrontal cortex, the striatum and the thalamus, as well as with previous evidence that dysfunction within these circuits plays a major role in the pathophysiology of BD (Strakowski et al. 2005). Fronto-limbic abnormalities in BD also have been supported from the view of FC by a number of task-based fMRI studies (de Almeida et al. 2009; Versace et al. 2010), but may be complex and difficult to be detected during resting-date (Stoddard et al. 2016; Vargas et al. 2013). A few FC studies that probe limbic regions directly found abnormal prefrontal-limbic connectivity in resting BD subjects (Anticevic et al. 2013; Chepenik et al. 2010; Torrisi et al. 2013). No significant group difference in fronto-limbic FC was observed in our previous FNC study on the same data set. Our results from the modular analysis performed herein on the FNC component thus may provide a more sensitive method for detecting prefrontal-limbic dysfunction in BD patients during rest.

GMD Abnormality in MDD

Beside the joint group-discriminative IC5, GMD-IC2 was identified as modality-specific group-discriminative IC, where group difference was only found in GMD. In our study, both BD and MDD exhibited higher mixing weights associated with GMD-IC2 compared to HC, but no statistical difference was detected between the patients in two disorders. The amygdale and anterior hippocampus form central structures of the limbic system and play major roles in emotion regulation, episodic memory, and responses to stressors, threats and appetitive stimuli (Aggleton 1992; Burgess et al. 2002). Consistent with their functional roles, deficits of amygdala related to mood disorders such as BD and MDD are widely supported from a variety of neuroimaging approaches (Price and Drevets 2012; Videbech 2000).

Although many structural studies on the BD group demonstrated reduced amygdala volume compared to healthy subjects (Blumberg et al. 2003; Foland-Ross et al. 2012; Phillips and Swartz 2014), other studies reported amygdala in BD were either enlarged (Haldane et al. 2008) or unchanged (Almeida et al. 2009). (Drevets 2003; Savitz et al. 2010) provided evidence that speculate the disagreement at least partly be explained by the putative neurotrophic / neuroprotective effects of some mood stabilizer treatments in BD. With medication effects controlled, Savitz et al. found amygdala volumes declined in unmedicated BD in contrast to HC (Savitz et al. 2010). Instead of selecting ROI a priori, our analysis approach was data-driven. The IC of gray matter density demonstrated similar trend of amygdala reduction in unmedicated BD compared to HC. However, the group difference did not reach statistical significance after FDR correction, potentially reflecting the biological heterogeneity within these phenotypes (Savitz et al. 2015a; Savitz et al. 2015b).

On the other hand, the reduction in amygdala volume in MDD appears generally consistent with a variety of recent analyses (Bora et al. 2012; Sacher et al. 2012; Tang et al. 2007; Zou et al. 2010), and our results that GMD-IC2 of MDD exhibits significant change compared to HC is in accordance with them. In addition to the amygdala abnormality, GMD-IC2 includes part of culmen and declive regions of the cerebellum as well. Simultaneous cerebellar and amygdala reduction in MDD was also reported in prior gray matter density studies (Lee et al. 2011; Peng et al. 2011). Recent studies have shown that the cerebellum plays a role in emotion regulation and cognition (Baldacara et al. 2008; Bugalho et al. 2006; Phillips et al. 2015), and also have implicated the cerebellum in MDD based on findings of altered structure (Yucel et al. 2013; Zhao et al. 2016) and function (Liu et al. 2012; Ma et al. 2013).

Classifications based on selected ICs

As an exploration, the group discriminative features extracted from multimodal analysis were evaluated using classification. Classifiers yielded highly accurate and reliable performance with cross-validation. Even though no significant difference was found between BD and MDD during statistical test on mixing profiles of individual ICs, classifiers still distinguished the two disorders with relatively high accuracy by combining the high-dimensional features from two modalities, indicating classification methods provide a mechanism for evaluating predictive power of the results which null hypothesis testing does not (Craddock et al. 2009). The classifiers trained with the combination of both modalities

performed better and more stable than those trained on a single modality, suggesting that information gained through multimodal fusion can improve the potential diagnostic prediction, in accordance with (Sui et al. 2009; Yang et al. 2010). These data merit replication in future studies to determine their potential utility as diagnostic biomarkers in mood disorders (Sui et al. 2013).

Limitations

Several methodological issues limit the conclusions that can be drawn from the current study. The major issue is the small number of subjects, especially in the BD group. In order to avoid the potential confound of medication, our study was limited to subjects who were treatment-naive or unmedicated for at least three weeks. However, this strict requirement constrained the sample size of this study. Nevertheless, most recent neuroimaging studies comparing BD and MDD reviewed in (de Almeida and Phillips 2013) also included sample sizes ranging from 10 to 30 subjects per patient group. During the evaluation of biomarkers with classification, we adopted an upsampling approach on the BD samples, in order to reduce the impact of the unbalanced group sizes on the classifiers. It would be helpful to increase statistical power by including more subjects in future studies. In addition, to utilize as much information as possible, the features were derived from all subjects. Although the classification models were tested with 10-fold cross validation, more solid conclusions can be drawn by examining the performance of biomarkers on new subjects which were excluded from the feature extraction process (Du et al. 2015; Meng et al. 2016).

Conclusion

In conclusion, we conducted fusion analysis on the functional network connectivity and gray matter density in mood disordered and healthy control samples, providing a novel perspective to neuroimaging abnormalities in mood disorders by combining both structural and functional MRI. Both multimodal and modality-specific discriminative components were detected. Comparing to HC, BD exhibited reduced GMD in the parietal and occipital cortices, which correlated with attenuated functional connectivity within sensory and motor networks as well as hyper-connectivity in regions that are putatively engaged in cognitive control. In addition, altered GMD features were found in MDD in the amygdala and cerebellum. High accuracy in discriminating across groups was achieved by trained classification models, implying that features extracted from our fusion analysis hold the potential to ultimately serve as diagnostic biomarkers in BD and MDD research.

Acknowledgments

This work is supported in part by the National Institute of Biomedical Imaging and Bioengineering (1R01EB006841 to Calhoun, VD), the National Institute of General Medical Sciences Center of Biomedical Research Excellence (COBRE) grant (P20GM103472 to Calhoun, VD), the “100 Talents Plan” of the Chinese Academy of Sciences (to Sui, J), and the Chinese Natural Science Foundation (No. 81471367 to Sui, J). Savitz, J and Victor, T received support from the William K. Warren Foundation.

References

Aggleton, JP. The amygdala : neurobiological aspects of emotion, memory, and mental dysfunction. Wiley-Liss; New York; Chichester: 1992.

Aha DW, Kibler D, Albert MK. Instance-Based Learning. Algorithms Mach Learn. 1991; 6:37–66. DOI: 10.1023/A:1022689900470

Allen EA, et al. A baseline for the multivariate comparison of resting-state networks. Frontiers in systems neuroscience. 2011; 5:2.doi: 10.3389/fnsys.2011.00002 [PubMed: 21442040]

Almeida JR, et al. Reduced gray matter volume in ventral prefrontal cortex but not amygdala in bipolar disorder: significant effects of gender and trait anxiety. Psychiatry Res. 2009; 171:54–68. DOI: 10.1016/j.pscychresns.2008.02.001 [PubMed: 19101126]

Anand A, Li Y, Wang Y, Lowe MJ, Dzemidzic M. Resting state corticolimbic connectivity abnormalities in unmedicated bipolar disorder and unipolar depression. Psychiat Res-Neuroim. 2009; 171:189–198. DOI: 10.1016/j.pscychresns.2008.03.012

Angst J, Cui L, Swendsen J, Rothen S, Cravchik A, Kessler RC, Merikangas KR. Major depressive disorder with subthreshold bipolarity in the National Comorbidity Survey Replication. Am J Psychiatry. 2010; 167:1194–1201. DOI: 10.1176/appi.ajp.2010.09071011 [PubMed: 20713498]

Anticevic A, et al. Global Prefrontal and Fronto-Amygdala Dysconnectivity. Bipolar I Disorder with Psychosis History Biol Psychiat. 2013; 73:565–573. DOI: 10.1016/j.biopsych.2012.07.031 [PubMed: 22980587]

Ashburner J, Friston KJ. Unified segmentation. NeuroImage. 2005; 26:839–851. doi:S1053-8119(05)00110-2 [pii]10.1016/j.neuroimage.2005.02.018. [PubMed: 15955494]

Baldacara L, Borgio JG, Lacerda AL, Jackowski AP. Cerebellum and psychiatric disorders. Rev Bras Psiquiatr. 2008; 30:281–289. [PubMed: 18833430]

Benjamini Y, Hochberg Y. Controlling the False Discovery Rate - a Practical and Powerful Approach to Multiple Testing. J Roy Stat Soc B Met. 1995; 57:289–300.

Biswal B, Yetkin FZ, Haughton VM, Hyde JS. Functional Connectivity in the Motor Cortex of Resting Human Brain Using Echo-Planar. Mri Magn Reson Med. 1995; 34:537–541. DOI: 10.1002/mrm.1910340409 [PubMed: 8524021]

Blumberg HP, et al. Amygdala and hippocampal volumes in adolescents and adults with bipolar disorder. Arch Gen Psychiat. 2003; 60:1201–1208. DOI: 10.1001/archpsyc.60.12.1201 [PubMed: 14662552]

Bora E, Fornito A, Pantelis C, Yucel M. Gray matter abnormalities in Major Depressive Disorder: a meta-analysis of voxel based morphometry studies. J Affect Disord. 2012; 138:9–18. DOI: 10.1016/j.jad.2011.03.049 [PubMed: 21511342]

Breiman L. Random forests. Mach Learn. 2001; 45:5–32. DOI: 10.1023/A:1010933404324

Bugalho P, Correa B, Viana-Baptista M. [Role of the cerebellum in cognitive and behavioural control: scientific basis and investigation models]. Acta Med Port. 2006; 19:257–267. [PubMed: 17234089]

Burgess N, Maguire EA, O'Keefe J. The human hippocampus and spatial and episodic memory. Neuron. 2002; 35:625–641. [PubMed: 12194864]

Calhoun VD, Adali T. Multisubject independent component analysis of fMRI: a decade of intrinsic networks, default mode, and neurodiagnostic discovery IEEE. Rev Biomed Eng. 2012; 5:60–73. DOI: 10.1109/RBME.2012.2211076

Calhoun VD, Adali T, Giuliani NR, Pekar JJ, Kiehl KA, Pearlson GD. Method for Multimodal analysis of independent source differences in schizophrenia: Combining gray matter structural and auditory oddball functional data. Human Brain Mapping. 2006; 27:47–62. DOI: 10.1002/hbm.20166 [PubMed: 16108017]

Calhoun VD, Sui J. Multimodal fusion of brain imaging data: A key to finding the missing link(s) in complex mental illness Biological Psychiatry: Cognitive. Neuroscience and Neuroimaging. 2016

Calhoun VD, Sui J, Kiehl K, Turner J, Allen E, Pearlson G. Exploring the psychosis functional connectome: aberrant intrinsic networks in schizophrenia and bipolar disorder. Front Psychiatry. 2011; 2:75.doi: 10.3389/fpsyt.2011.00075 [PubMed: 22291663]

Cerullo MA, et al. Bipolar I disorder and major depressive disorder show similar brain activation during depression. Bipolar Disord. 2014; 16:703–712. DOI: 10.1111/bdi.12225 [PubMed: 24990479]

Chawla NV, Bowyer KW, Hall LO, Kegelmeyer WP. SMOTE: Synthetic minority over-sampling technique. J Artif Intell Res. 2002; 16:321–357.

Chepenik LG, et al. Functional connectivity between ventral prefrontal cortex and amygdala at low frequency in the resting state in bipolar disorder. Psychiat Res-Neuroim. 2010; 182:207–210. DOI: 10.1016/j.pscychresns.2010.04.002

Craddock RC, Holtzheimer PE 3rd, Hu XP, Mayberg HS. Disease state prediction from resting state functional connectivity. Magn Reson Med. 2009; 62:1619–1628. DOI: 10.1002/mrm.22159 [PubMed: 19859933]

de Almeida JRC, Phillips ML. Distinguishing between Unipolar Depression and Bipolar Depression: Current and Future Clinical and Neuroimaging Perspectives. Biol Psychiat. 2013; 73:111–118. DOI: 10.1016/j.biopsych.2012.06.010 [PubMed: 22784485]

de Almeida JRC, Versace A, Mechelli A, Hassel S, Quevedo K, Kupfer DJ, Phillips ML. Abnormal Amygdala-Prefrontal Effective Connectivity to Happy Faces Differentiates Bipolar from Major Depression. Biol Psychiat. 2009; 66:451–459. DOI: 10.1016/j.biopsych.2009.03.024 [PubMed: 19450794]

Delvecchio G, et al. Common and distinct neural correlates of emotional processing in Bipolar Disorder and Major Depressive Disorder: a voxel-based meta-analysis of functional magnetic resonance imaging studies. European neuropsychopharmacology : the journal of the European College of Neuropsychopharmacology. 2012; 22:100–113. DOI: 10.1016/j.euroneuro.2011.07.003 [PubMed: 21820878]

Doris A, Belton E, Ebmeier KP, Glabus MF, Marshall I. Reduction of cingulate gray matter density in poor outcome bipolar illness. Psychiatry Res. 2004; 130:153–159. DOI: 10.1016/j.pscychresns.2003.09.002 [PubMed: 15033185]

Drevets WC. Neuroimaging studies of mood disorders. Biol Psychiat. 2000; 48:813–829. DOI: 10.1016/S0006-3223(00)01020-9 [PubMed: 11063977]

Drevets WC. Neuroimaging abnormalities in the amygdala in mood disorders. Ann N Y Acad Sci. 2003; 985:420–444. [PubMed: 12724175]

Du YH, et al. A group ICA based framework for evaluating resting fMRI markers when disease categories are unclear: application to schizophrenia, bipolar, and schizoaffective disorders. Neuroimage. 2015; 122:272–280. DOI: 10.1016/j.neuroimage.2015.07.054 [PubMed: 26216278]

Ellard K, et al. Resting-State Functional Connectivity of Anterior Insula Differentiates Bipolar and Unipolar Depression. Neuropsychopharmacol. 2015; 40:S496–S497.

Ferrier IN, Chowdhury R, Thompson JM, Watson S, Young AH. Neurocognitive function in unaffected first-degree relatives of patients with bipolar disorder: a preliminary report. Bipolar Disord. 2004; 6:319–322. [PubMed: 15225150]

Foland-Ross LC, Brooks JO, Mintz J, Bartzokis G, Townsend J, Thompson PM, Altshuler LL. Mood-state effects on amygdala volume in bipolar disorder. J Affect Disord. 2012; 139:298–301. DOI: 10.1016/j.jad.2012.03.003 [PubMed: 22521854]

Frazier JA, et al. Cortical gray matter differences identified by structural magnetic resonance imaging in pediatric bipolar disorder. Bipolar Disord. 2005; 7:555–569. DOI: 10.1111/j.1399-5618.2005.00258.x [PubMed: 16403181]

Freire L, Roche A, Mangin JF. What is the best similarity measure for motion correction in fMRI time series? IEEE. Trans Med Imaging. 2002; 21:470–484. DOI: 10.1109/TMI.2002.1009383

Friston KJ. Beyond phrenology: What can neuroimaging tell us about distributed circuitry? Annu Rev Neurosci. 2002; 25:221–250. DOI: 10.1146/annurev.neuro.25.112701.142846 [PubMed: 12052909]

Goya-Maldonado R, Brodmann K, Keil M, Trost S, Dechent P, Gruber O. Differentiating Unipolar and Bipolar Depression by Alterations in Large-Scale Brain Networks. Human Brain Mapping. 2016; 37:808–818. DOI: 10.1002/hbm.23070 [PubMed: 26611711]

Greicius MD, Supekar K, Menon V, Dougherty RF. Resting-State Functional Connectivity Reflects Structural Connectivity in the Default Mode Network. Cereb Cortex. 2009; 19:72–78. DOI: 10.1093/cercor/bhn059 [PubMed: 18403396]

Guimera R, Amaral LAN. Functional cartography of complex metabolic networks. Nature. 2005; 433:895–900. DOI: 10.1038/nature03288 [PubMed: 15729348]

Haldane M, Cunningham G, Androutsos C, Frangou S. Structural brain correlates of response inhibition in Bipolar Disorder. I J Psychopharmacol. 2008; 22:138–143. DOI: 10.1177/0269881107082955 [PubMed: 18308812]

He H, et al. Resting-state functional network connectivity in prefrontal regions differs between unmedicated patients with bipolar and major depressive disorders. J Affect Disord. 2016; 190:483–493. DOI: 10.1016/j.jad.2015.10.042 [PubMed: 26551408]

Jafri MJ, Pearlson GD, Stevens M, Calhoun VD. A method for functional network connectivity among spatially independent resting-state components in schizophrenia. Neuroimage. 2008; 39:1666–1681. DOI: 10.1016/j.neuroimage.2007.11.001 [PubMed: 18082428]

Jie NF, et al. Discriminating Bipolar Disorder From Major Depression Based on SVM-FoBa: Efficient Feature Selection With Multimodal Brain Imaging Data Ieee. T Auton Ment De. 2015; 7:320–331. DOI: 10.1109/Tamd.2015.2440298

John, HGL. Eleventh Conference on Uncertainty in Artificial Intelligence. San Mateo: 1995. P Estimating Continuous Distributions in Bayesian Classifiers; p. 338-345.

Judd LL, et al. Prevalence and clinical significance of subsyndromal manic symptoms, including irritability and psychomotor agitation, during bipolar major depressive episodes. J Affect Disord. 2012; 138:440–448. DOI: 10.1016/j.jad.2011.12.046 [PubMed: 22314261]

Keerthi SS, Shevade SK, Bhattacharyya C, Murthy KRK. Improvements to Platt's SMO algorithm for SVM classifier design. Neural Comput. 2001; 13:637–649. DOI: 10.1162/089976601300014493

Kempton MJ, Salvador Z, Munafo MR, Geddes JR, Simmons A, Frangou S, Williams SC. Structural neuroimaging studies in major depressive disorder. Meta-analysis and comparison with bipolar disorder. Arch Gen Psychiat. 2011; 68:675–690. DOI: 10.1001/archgenpsychiatry.2011.60 [PubMed: 21727252]

Konarski JZ, Mcintyre RS, Kennedy SH, Rafi-Tari S, Soczynska JK, Ketter TA. Volumetric neuroimaging investigations in mood disorders: bipolar disorder versus major depressive disorder. Bipolar Disord. 2008; 10:1–37.

Kupfer DJ, Frank E, Phillips ML. Major depressive disorder: new clinical, neurobiological, and treatment perspectives. Lancet. 2012; 379:1045–1055. DOI: 10.1016/S0140-6736(11)60602-8 [PubMed: 22189047]

Lancet. Global, regional, and national age-sex specific all-cause and cause-specific mortality for 240 causes of death, 1990–2013: a systematic analysis for the Global Burden of Disease Study 2013. Lancet. 2015; 385:117–171. DOI: 10.1016/S0140-6736(14)61682-2 [PubMed: 25530442]

Lee HY, et al. Demonstration of decreased gray matter concentration in the midbrain encompassing the dorsal raphe nucleus and the limbic subcortical regions in major depressive disorder: an optimized voxel-based morphometry study. J Affect Disord. 2011; 133:128–136. DOI: 10.1016/j.jad.2011.04.006 [PubMed: 21546094]

Li YO, Adali T, Calhoun VD. Estimating the number of independent components for functional magnetic resonance imaging data. Hum Brain Mapp. 2007; 28:1251–1266. [PubMed: 17274023]

Li YO, Adali T, Wang W, Calhoun VD. Joint Blind Source Separation by Multi-set Canonical Correlation Analysis IEEE. Trans Signal Process. 2009; 57:3918–3929. DOI: 10.1109/TSP.2009.2021636

Liu L, Zeng LL, Li Y, Ma Q, Li B, Shen H, Hu D. Altered cerebellar functional connectivity with intrinsic connectivity networks in adults with major depressive disorder. PLoS ONE. 2012; 7:e39516.doi: 10.1371/journal.pone.0039516 [PubMed: 22724025]

Lochhead RA, Parsey RV, Oquendo MA, Mann JJ. Regional brain gray matter volume differences in patients with bipolar disorder as assessed by optimized voxel-based morphometry. Biol Psychiat. 2004; 55:1154–1162. DOI: 10.1016/j.biopsych.2004.02.026 [PubMed: 15184034]

Lyoo IK, et al. Frontal lobe gray matter density decreases in bipolar I disorder. Biol Psychiat. 2004; 55:648–651. DOI: 10.1016/j.biopsych.2003.10.017 [PubMed: 15013835]

Lyoo IK, et al. Regional cerebral cortical thinning in bipolar disorder. Bipolar Disord. 2006; 8:65–74. DOI: 10.1111/j.1399-5618.2006.00284.x [PubMed: 16411982]

Ma Q, Zeng LL, Shen H, Liu L, Hu D. Altered cerebellar-cerebral resting-state functional connectivity reliably identifies major depressive disorder. Brain Res. 2013; 1495:86–94. DOI: 10.1016/j.brainres.2012.12.002 [PubMed: 23228724]

Marchand WR, Lee JN, Johnson S, Gale P, Thatcher J. Differences in functional connectivity in major depression versus bipolar II depression. J Affect Disord. 2013; 150:527–532. DOI: 10.1016/j.jad.2013.01.028 [PubMed: 23433856]

Mars RB, et al. Diffusion-Weighted Imaging Tractography-Based Parcellation of the Human Parietal Cortex and Comparison with Human and Macaque Resting-State Functional Connectivity. Journal of Neuroscience. 2011; 31:4087–4100. DOI: 10.1523/Jneurosci.5102-10.2011 [PubMed: 21411650]

Meng X, et al. Predicting individualized clinical measures by a generalized prediction framework and multimodal fusion of MRI data. Neuroimage. 2016; doi: 10.1016/j.neuroimage.2016.05.026

Nolte, J. The human brain : an introduction to its functional anatomy. 6. Mosby/Elsevier; Philadelphia, PA: 2009.

Ongur D, Lundy M, Greenhouse I, Shinn AK, Menon V, Cohen BM, Renshaw PF. Default mode network abnormalities in bipolar disorder and schizophrenia. Psychiat Res-Neuroim. 2010; 183:59–68. DOI: 10.1016/j.pscychresns.2010.04.008

Park B, Kim DS, Park HJ. Graph independent component analysis reveals repertoires of intrinsic network components in the human brain. PLoS ONE. 2014; 9:e82873.doi: 10.1371/journal.pone.0082873 [PubMed: 24409279]

Passarotti AM, Ellis J, Wegbreit E, Stevens MC, Pavuluri MN. Reduced functional connectivity of prefrontal regions and amygdala within affect and working memory networks in pediatric bipolar disorder. Brain Connect. 2012; 2:320–334. DOI: 10.1089/brain.2012.0089 [PubMed: 23035965]

Peng J, Liu J, Nie B, Li Y, Shan B, Wang G, Li K. Cerebral and cerebellar gray matter reduction in first-episode patients with major depressive disorder: a voxel-based morphometry study. Eur J Radiol. 2011; 80:395–399. DOI: 10.1016/j.ejrad.2010.04.006 [PubMed: 20466498]

Phillips JR, Hewedi DH, Eissa AM, Moustafa AA. The cerebellum and psychiatric disorders. Front Public Health. 2015; 3:66.doi: 10.3389/fpubh.2015.00066 [PubMed: 26000269]

Phillips M, Ladouceur C, Drevets W. A neural model of voluntary and automatic emotion regulation: implications for understanding the pathophysiology and neurodevelopment of bipolar disorder. Mol Psychiatr. 2008; 13:833–857. DOI: 10.1038/mp.2008.65

Phillips ML, Swartz HA. A critical appraisal of neuroimaging studies of bipolar disorder: toward a new conceptualization of underlying neural circuitry and a road map for future research. Am J Psychiatry. 2014; 171:829–843. DOI: 10.1176/appi.ajp.2014.13081008 [PubMed: 24626773]

Poldrack RA. Mapping Mental Function to Brain Structure: How Can Cognitive Neuroimaging Succeed? Perspect Psychol Sci. 2010; 5:753–761. DOI: 10.1177/1745691610388777 [PubMed: 25076977]

Price JL, Drevets WC. Neural circuits underlying the pathophysiology of mood disorders. Trends in Cognitive Sciences. 2012; 16:61–71. DOI: 10.1016/j.tics.2011.12.011 [PubMed: 22197477]

Redlich R, et al. Reward Processing in Unipolar and Bipolar Depression: A Functional MRI Study. Neuropsychopharmacol. 2015; 40:2623–2631. DOI: 10.1038/npp.2015.110

Reichardt J, Bornholdt S. Statistical mechanics of community detection. Phys Rev E. 2006:74. doi: Artn 01611010.1103/Physreve.74.016110.

Rigucci S, Serafini G, Pompili M, Kotzalidis GD, Tatarelli R. Anatomical and functional correlates in major depressive disorder: the contribution of neuroimaging studies. World J Biol Psychiatry. 2010; 11:165–180. DOI: 10.1080/15622970903131571 [PubMed: 19670087]

Ronhovde P, Nussinov Z. Multiresolution community detection for megascale networks by information-based replica correlations. Phys Rev E. 2009; 80 doi: Artn 01610910.1103/Physreve.80.016109.

Rubinov M, Sporns O. Complex network measures of brain connectivity: uses and interpretations. Neuroimage. 2010; 52:1059–1069. DOI: 10.1016/j.neuroimage.2009.10.003 [PubMed: 19819337]

Sacher J, Neumann J, Funfstuck T, Soliman A, Villringer A, Schroeter ML. Mapping the depressed brain: a meta-analysis of structural and functional alterations in major depressive disorder. J Affect Disord. 2012; 140:142–148. DOI: 10.1016/j.jad.2011.08.001 [PubMed: 21890211]

Salomon JA, Wang H, Freeman MK, Vos T, Flaxman AD, Lopez AD, Murray CJ. Healthy life expectancy for 187 countries, 1990–2010: a systematic analysis for the Global Burden Disease

Study 2010. Lancet. 2012; 380:2144–2162. DOI: 10.1016/S0140-6736(12)61690-0 [PubMed: 23245606]

Satterthwaite TD, et al. Common and Dissociable Dysfunction of the Reward System in Bipolar and Unipolar Depression. Neuropsychopharmacol. 2015; 40:2258–2268. DOI: 10.1038/npp.2015.75

Savitz J, et al. Neuroprotective kynurenine metabolite indices are abnormally reduced and positively associated with hippocampal and amygdalar volume in bipolar disorder. Psychoneuroendocrinology. 2015a; 52:200–211. DOI: 10.1016/j.psyneuen.2014.11.015 [PubMed: 25486577]

Savitz J, et al. Putative neuroprotective and neurotoxic kynurenine pathway metabolites are associated with hippocampal and amygdalar volumes in subjects with major depressive disorder. Neuropsychopharmacology : official publication of the American College of Neuropsychopharmacology. 2015b; 40:463–471. DOI: 10.1038/npp.2014.194 [PubMed: 25074636]

Savitz J, et al. Amygdala volume in depressed patients with bipolar disorder assessed using high resolution 3T MRI: The impact of medication. Neuroimage. 2010; 49:2966–2976. DOI: 10.1016/j.neuroimage.2009.11.025 [PubMed: 19931399]

Stoddard J, et al. Aberrant intrinsic functional connectivity within and between corticostriatal and temporal-parietal networks in adults and youth with bipolar disorder. Psychological Medicine. 2016; 46:1509–1522. DOI: 10.1017/S0033291716000143 [PubMed: 26924633]

Strakowski SM, DelBello MP, Adler CM. The functional neuroanatomy of bipolar disorder: a review of neuroimaging findings. Mol Psychiatr. 2005; 10:105–116. DOI: 10.1038/sj.mp.4001585

Sui J, Adali T, Pearlson G, Yang HH, Sponheim SR, White T, Calhoun VD. A CCA plus ICA based model for multi-task brain imaging data fusion and its application to schizophrenia. Neuroimage. 2010; 51:123–134. DOI: 10.1016/j.neuroimage.2010.01.069 [PubMed: 20114081]

Sui J, Adali T, Pearlson GD, Calhoun VD. An ICA-based method for the identification of optimal FMRI features and components using combined group-discriminative techniques. Neuroimage. 2009; 46:73–86. DOI: 10.1016/j.neuroimage.2009.01.026 [PubMed: 19457398]

Sui J, Adali T, Yu QB, Chen JY, Calhoun VD. A review of multivariate methods for multimodal fusion of brain imaging data. J Neurosci Methods. 2012a; 204:68–81. DOI: 10.1016/j.jneumeth.2011.10.031 [PubMed: 22108139]

Sui J, et al. Three-way (N-way) fusion of brain imaging data based on mCCA+jICA and its application to discriminating schizophrenia. Neuroimage. 2012b; doi: 10.1016/j.neuroimage.2012.10.051

Sui J, et al. Combination of resting state fMRI, DTI, and sMRI data to discriminate schizophrenia by N-way MCCA plus jICA. Front Hum Neurosci 7. 2013 doi: Artn 23510.3389/Fnhum.2013.00235.

Sui J, et al. In Search of Multimodal Neuroimaging Biomarkers of Cognitive Deficits in Schizophrenia. Biol Psychiat. 2015; 78:794–804. DOI: 10.1016/j.biopsych.2015.02.017 [PubMed: 25847180]

Sweeney JA, Kmiec JA, Kupfer DJ. Neuropsychologic impairments in bipolar and unipolar mood disorders on the CANTAB neurocognitive battery. Biol Psychiat. 2000; 48:674–684. DOI: 10.1016/S0006-3223(00)00910-0 [PubMed: 11032979]

Tang Y, et al. Reduced ventral anterior cingulate and amygdala volumes in medication-naive females with major depressive disorder: A voxel-based morphometric magnetic resonance imaging study. Psychiatry Res. 2007; 156:83–86. DOI: 10.1016/j.pscychresns.2007.03.005 [PubMed: 17825533]

Torrisi S, et al. Differences in resting corticolimbic functional connectivity in bipolar I euthymia. Bipolar Disord. 2013; 15:156–166. DOI: 10.1111/bdi.12047 [PubMed: 23347587]

van den Heuvel MP, Mandl RCW, Kahn RS, Pol HEH. Functionally Linked Resting-State Networks Reflect the Underlying Structural Connectivity Architecture of the Human Brain. Human Brain Mapping. 2009; 30:3127–3141. DOI: 10.1002/hbm.20737 [PubMed: 19235882]

Van Essen DC, Dierker D. On navigating the human cerebral cortex: Response to ‘in praise of tedious anatomy’. Neuroimage. 2007; 37:1050–1054. DOI: 10.1016/j.neuroimage.2007.02.021 [PubMed: 17766148]

Vargas C, Lopez-Jaramillo C, Vieta E. A systematic literature review of resting state network-functional MRI in bipolar disorder. J Affect Disord. 2013; 150:727–735. DOI: 10.1016/j.jad.2013.05.083 [PubMed: 23830141]

Versace A, et al. Abnormal Left and Right Amygdala-Orbitofrontal Cortical Functional Connectivity to Emotional Faces: State Versus Trait Vulnerability Markers of Depression in Bipolar Disorder. Biol Psychiat. 2010; 67:422–431. DOI: 10.1016/j.biopsych.2009.11.025 [PubMed: 20159144]

Videbech P. PET measurements of brain glucose metabolism and blood flow in major depressive disorder: a critical review. Acta Psychiatr Scand. 2000; 101:11–20. [PubMed: 10674946]

Wang Y, Zhong SM, Jia YB, Zhou ZF, Wang B, Pan JY, Huang L. Interhemispheric resting state functional connectivity abnormalities in unipolar depression and bipolar depression. Bipolar Disord. 2015; 17:486–495. DOI: 10.1111/bdi.12315 [PubMed: 26241359]

White T, O'Leary D, Magnotta V, Arndt S, Flaum M, Andreasen NC. Anatomic and functional variability: the effects of filter size in group fMRI data analysis. Neuroimage. 2001; 13:577–588. doi:10.1006/nimg.2000.0716S1053-8119(00)90716-X [pii]. [PubMed: 11305887]

Witten IH, Frank E, Hall MA. Introduction to Weka. Mor Kauf D. 2011; :403–406. DOI: 10.1016/B978-0-12-374856-0.00010-9

Xia M, Wang J, He Y. BrainNet Viewer: a network visualization tool for human brain connectomics. PLoS ONE. 2013; 8:e68910.doi: 10.1371/journal.pone.0068910 [PubMed: 23861951]

Xu L, Groth KM, Pearlson G, Schretlen DJ, Calhoun VD. Source-Based Morphometry: The Use of Independent Component Analysis to Identify Gray Matter Differences With Application to Schizophrenia. Human Brain Mapping. 2009; 30:711–724. DOI: 10.1002/hbm.20540 [PubMed: 18266214]

Yang HH, Liu JY, Sui J, Pearlson G, Calhoun VD. A hybrid machine learning method for fusing fMRI and genetic data: combining both improves classification of schizophrenia. Front Hum Neurosci. 2010:4. doi: Artn 19210.3389/Fnhum.2010.00192. [PubMed: 20198130]

Yu Q, et al. Modular Organization of Functional Network Connectivity in Healthy Controls and Patients with Schizophrenia during the Resting State. Frontiers in systems neuroscience. 2011; 5:103.doi: 10.3389/fnsys.2011.00103 [PubMed: 22275887]

Yucel K, Nazarov A, Taylor VH, Macdonald K, Hall GB, Macqueen GM. Cerebellar vermis volume in major depressive disorder. Brain Struct Funct. 2013; 218:851–858. DOI: 10.1007/s00429-012-0433-2 [PubMed: 22696069]

Zhao LP, et al. Cerebellar microstructural abnormalities in bipolar depression and unipolar depression: A diffusion kurtosis and perfusion imaging study. J Affect Disord. 2016; 195:21–31. DOI: 10.1016/j.jad.2016.01.042 [PubMed: 26852094]

Zou K, Deng W, Li T, Zhang B, Jiang L, Huang C, Sun X. Changes of brain morphometry in first-episode, drug-naive, non-late-life adult patients with major depression: an optimized voxel-based morphometry study. Biol Psychiat. 2010; 67:186–188. DOI: 10.1016/j.biopsych.2009.09.014 [PubMed: 19897176]

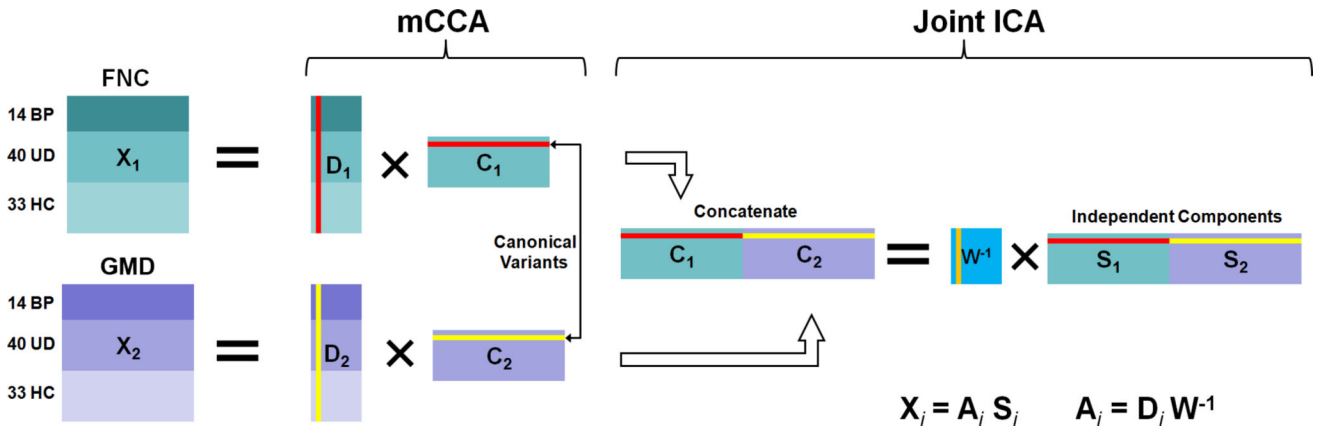

Figure 1.
The overall procedure of mCCA+jICA multimodal fusion on FNC and GMD

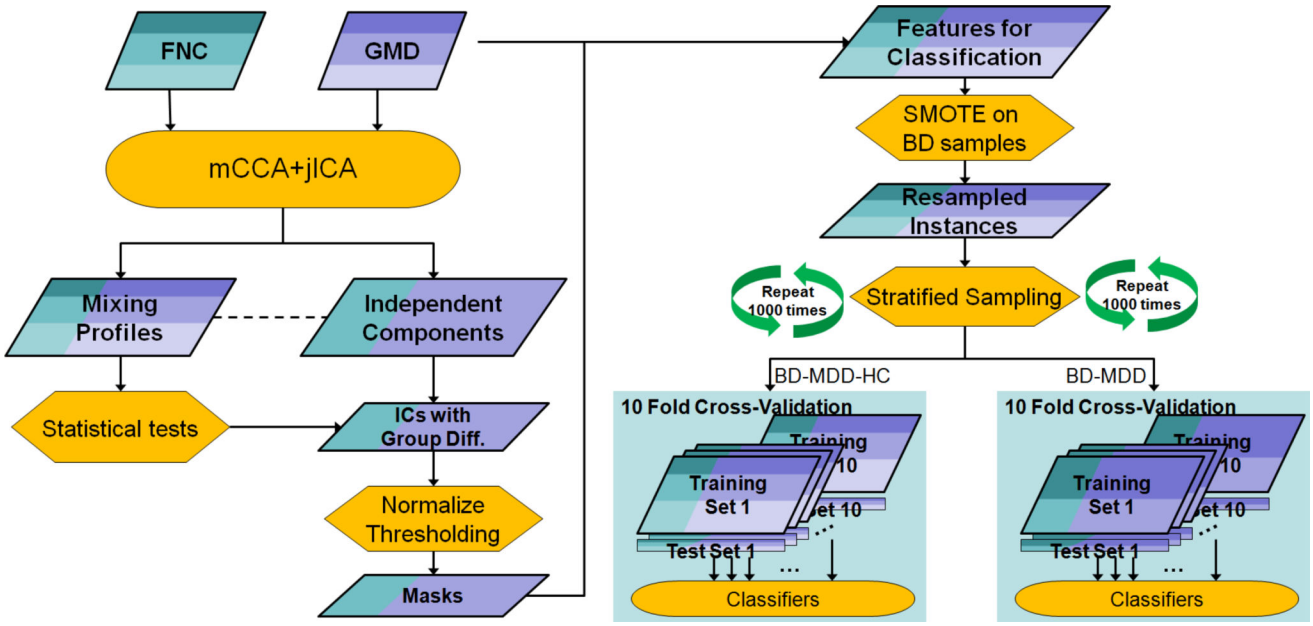

Figure 2.
Flowchart of disease classification with components derived from multimodal fusion.

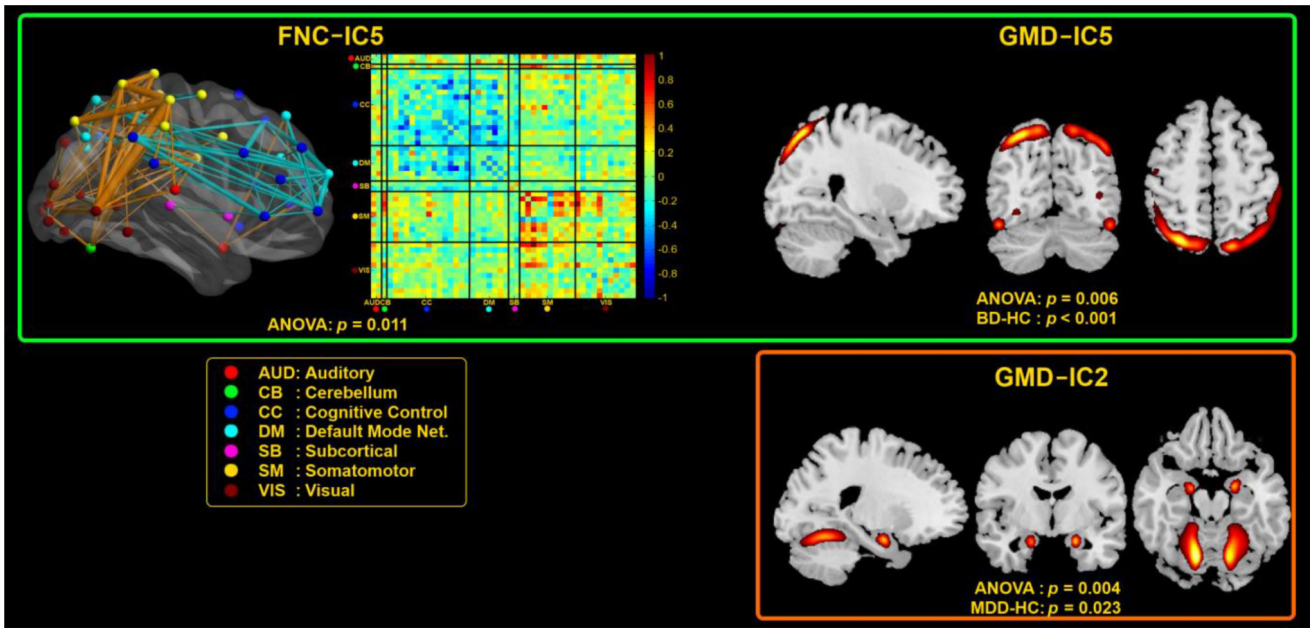

Figure 3.

IC5 demonstrated significant group differences in both FNC (top left) and GMD (top right). IC2 showed a significant group difference in GMD only (bottom). In FNC-IC5, the nodes correspond to intrinsic connectivity networks (ICNs), and the links are edges of the subnetwork between node-pairs. Thickness of links represent to connectivity weights of the subnetwork. Only the top 10% weighted links are displayed for clearer visualization. Orange links indicate the weights are positively correlated with the mixing profile of FNC-IC5, while green links indicate the weights are negatively correlated with mixing profile of FNC-IC5.

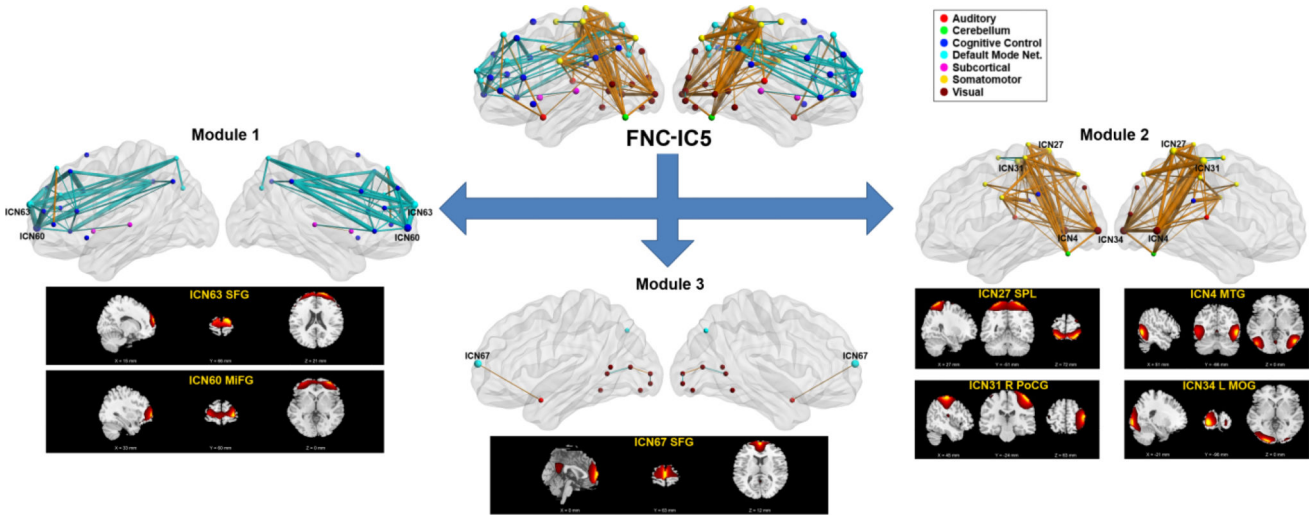

Figure 4.

Forty-eight ICNs in the subnetwork FNC-IC5 can be divided into three modules. Hubs nodes in each module are enlarged and labeled. There were two hubs in Module 1, four hubs in Module 2, and one hub in Module 3. Only top 10% weighted links are displayed for better visualizing purposes. Orange links indicate the weights are positively correlated with the mixing profile of FNC-IC5, while green links indicate the weight are negatively correlated with mixing profile of FNC-IC5.

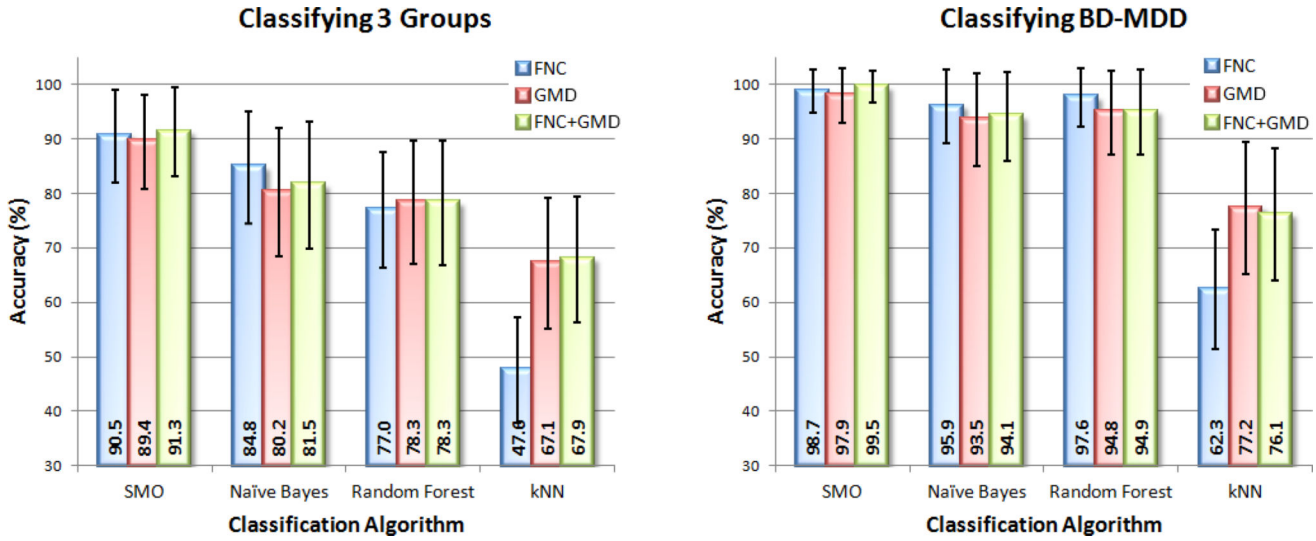

Figure 5.

Performance of classification algorithms that discriminated the 3 groups (left) and BD vs. MDD (right), depicted as mean and standard deviation of the accuracy from each of four classifiers trained with features extracted from fusion analysis.

Table 1

Demographic and clinical characteristics of the subject samples

	BD	MDD	HC	*p*-value
N (Females)	13 (11)	40 (33)	33 (22)	0.22 (chi-square)
Ages	35.15 ± 10.29	35.20 ± 9.31	33.70 ± 10.15	0.84 (ANOVA)
YMRS	6.15 ± 6.11	3.59 ± 2.33	0.16 ± 0.51	<0.001 (ANOVA)
MADRS	24.92 ± 10.31	30.90 ± 6.31	0.73 ± 1.72	<0.001 (ANOVA) 0.0151 (t-test, BD-MDD)

BD: bipolar disorder group; MDD: major depressive disorder group; HC: healthy controls group. YMRS: Young Mania Rating Scale; MADRS: Montgomery-Åsberg Depression Rating Scale.